



Waste Heat Conversion to Power via Organic Rankine Cycle

Mohamed. Aissa

Faculty of Engineering (Garbolli),
Elmergib University
maaisa@elmergib.edu.ly

Fawzi. Elhamshri

Faculty of Engineering (Garbolli),
Elmergib University
elhamshrifawzi@gmail.com

Hana. Elshafu

Faculty of Art and Science (Gaser
Alkhyaar), Elmergib University
helshafu@yahoo.com

Abstract— several studies have been carried out on how to recover waste heat using Organic Rankine cycle. Each study applied different working conditions, power scale and cycle configuration, hence an assessment of working fluids is given for specific case. As a result, no single working fluid have been identified that would meet an entire heat source temperature levels. This motivated us to examine various substances for use as working fluids for subcritical ORC systems operating in the temperature range (543 - 633K). In this study, with a given finite thermal source, performance of working fluid candidates are evaluated and assessed using four criteria: thermal efficiency, exergy efficiency, total exergy destruction and net power output. Results of the study indicate that from a performance point of view, the linear alkanes such as nonane seem to be a suitable fluid in the temperature range (543-573K). Beyond aforementioned temperature range it appears that aromatic hydrocarbons such as toluene, ethylbenzene, P-xylene, O-xylene, propylbenzene performed better. Under this condition, they represent comparably similar proposed screening criteria parameters and comparably high evaporating pressure, with only occasional slight differences between them.

Index Terms: Waste Heat Recovery, Organic Rankine Cycle, Subcritical Cycle, Modeling and Optimization.

I. INTRODUCTION

In the industrial and daily processes, an abundant source of emission-free power is rejected as a waste heat during normal operation, much of which is finally discharged into the environment, either to water or to the atmosphere. This amount of unused wasted heat, which is available at different temperature levels, contributes to serious environmental pollution such as global warming, ozone layer destruction, acid rain, water pollution and land pollution[1]. In this context, the desire to recover and re-use of waste heat sources more efficiently has led recently to an increased interest in developing an efficient technology that transforms waste heat into electricity.

Hence, ORC has emerged as a promising technology in future conservation energy and energy demands, by exploiting unused wasted heat into electricity[2]. One of the challenges of ORC is the selection of organic working fluid, it represents the main difference between ORCs and steam rankine cycle and is considered to be significantly important in maximizing the ORC overall efficiency[3]. The working fluids could be employed as pure or mixed fluids. To this purpose, the heat source at different temperature levels and the application influence significantly the proper selection of fluids and appropriate operating conditions [4]. Particularly, ORC is a key technology adopted to recover heat from various sources, both at low and at medium or high temperature. Although the majority of the existing articles have focused on the application of ORC and suitability of different working fluids, there are fewer studies examining heat recovery applications for high grade temperature sources. Ref.[5] conducted a detailed performance study to compare performances of hydrocarbons (C5 to C12) water, benzene and toluene for the waste heat sources with different temperature ranges. Their results showed that toluene and *n*-dodecane are more appropriate fluids for ORC systems when the heat is available at temperature of 773.15 K. In a case where heat is available at 623.15 K, toluene, *n*-octane, and water are more suitable choice.

Ref. [6] conducted a detailed performance study by employing ten aromatic hydrocarbons and siloxanes as potential working fluids in order to improve temperature matching and to generate power using intermediate and high temperature finite heat sources. Results from this study could be summarized as aromatic hydrocarbon are more suitable fluids for the ORC due to higher power output and less complex turbine design. The advantages of using mixed working fluids for ORCs were highlighted by [7]. They conducted a study starting with mixtures of siloxanes and hydrocarbons in comparison to pure working fluid for the waste heat sources with different temperature ranges. Their analysis was classified based on the cycle configurations into saturated, superheated and supercritical cycle, and the type of molecules as simple molecules and complex

Received 31 Oct, 2021; revised 20 Nov, 2021; accepted 20 Nov, 2021.

Available online 26 Nov, 2021.

molecules. They concluded that mixed composition fluids provide better temperature matching with the heat and cooling source. However, this leads to reduce the mean temperature difference between the heat source and working fluid in heat exchangers. This reduction implies that a higher heat exchanger area is required for a given heat flow, suggesting a trade-off between operating and capital costs[8].

Ref .[9] proposed a single objective function to maximize the thermal efficiency of the cycle, based on 1 MW of heat source.Their investigation was carried out with Simulated Annealing technique within the temperature range from 100 °C to 250 °C for the heat source and 30 °C for the heat sink.. The conclusion could be summarized as pure component organic fluids provide more energy-efficient than mixed organic fluids do. The conclusion could be summarized as pure component organic fluids provide more energy-efficient than mixed organic fluids do.

Although several studies have been carried out with different boundary conditions in order to identify the most suitable working fluid candidates to either low temperature waste heat sources up to 500 K or high temperature waste heat sources above 600 K, the results of these studies would not provide a reasonable assessment since each study applied different working condition power scale and cycle configuration [10, 11]. Therefore, no single potential working fluid could be identified that would meet the entire heat source temperature levels[3, 4]. Thus, a detailed working fluid selection study has to be taken into consideration for particular source temperature[12, 13]. In addition, the selected objective function of optimization has to be chosen depending on whether the selection of working fluid and process design considerations are based on maximizing the net power output , economical profitability, or on environmental considerations[14, 15]. This motivated us to examine various substances for use as working fluids for ORC systems operating at varied inlet temperatures which ranged from 543 K to 633K. In this study, finite thermal source is given and heat sink condition, performance of working fluid candidates are assessed using four criteria such as thermal efficiency, exergy efficiency, total exergy destruction and net power output.

according to the shape of the saturated vapor curve [9]. This property is the most important characteristics of the working fluid in an ORC cycle, because it affects applicability of working fluid in given temperature range and cycle efficiency. According to the T-S diagram in Figure. 1, the working fluid can be classified into three different groups. Those are dry, wet, or isentropic for positive, negative or nearly infinitely large slope respectively[3]. With reference to high temperature applications, the wet fluids are not recommended for subcritical cycle since they become saturated once they pass through a large enthalpy drop after generating power in the turbine, resulting in a shorter life of a turbine in ORC system [1]. On the other hand, dry and isentropic fluids have been proposed by researchers as a promising working fluid in an ORC for a high temperature finite heat source. Moreover, they do not pass through a distinct two-phase region, resulting in a better life of a turbine. However, beside essential thermo-physical properties that match the application, proper fluid must possess sufficient chemical stability over the desired operational temperature range. Assessing by thermodynamic characteristics, the most practical working fluids in the scopes of the temperature for studied case are siloxanes and hydrocarbons [16-18]. The working fluid candidates and their thermo-physical properties are listed in the Table. 1.

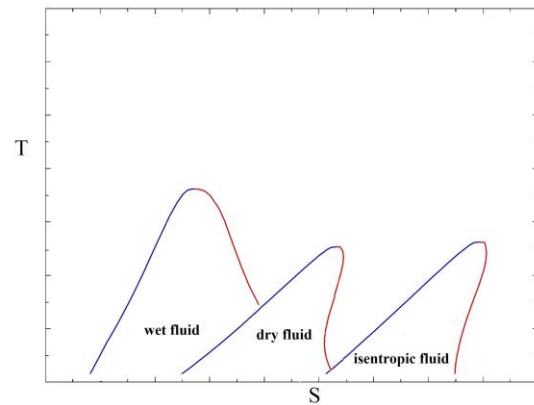


Figure. 1 T-S diagram of different types of working fluid.

Table. 1 Properties of working fluids.

Working fluid	Types of fluid	Critical point		
		T _c (K)	P _c (kPa)	V _c (m ³ /Kmol)
Ethylbenzene	dry	617.2	3609	0.37
N-nonane	dry	594.6	2290	0.55
O-Xylene	dry	630.3	3732	0.37
N-propylbenzene	dry	638.4	3200	0.44
p-Xylene	dry	616.2	3511	0.38
Toluene	Isentropic	591.8	4108	0.32

II. THERMODYNAMIC ANALYSIS

The ORC cycle consists of heat exchangers, a turbine, a condenser and a pump. It can be either subcritical or supercritical according to the state of working fluid at turbine inlet. An ORC cycle considered in this study is subcritical cycle. This type of an ORC can be categorized

In

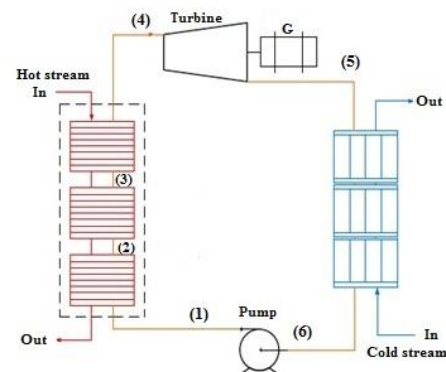


Figure. 2, a heat carrier fluid is characterized with a mass flow rate, inlet temperature, and outlet temperature. The heat carrier fluid, which is considered in this study as a

representative fluid, is flue gas. The stream of flue gas carrying heat source enters the system through three-zone heat exchangers, in which heat is transferred to the working fluid. Starting from state 2, the working fluid is heated in a pre-heater, where the temperature of the

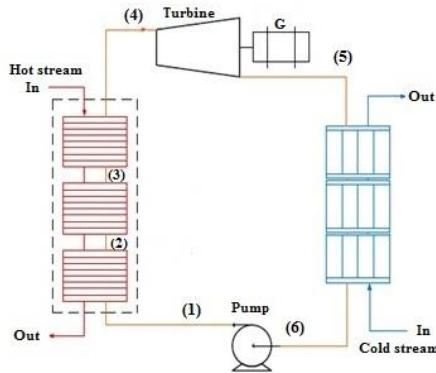


Figure. 2 Schematic diagram of the subcritical organic rankine cycle

working fluid is raised to its bubble point. Then, it is heated in the evaporator until it is vaporized and becomes saturated vapor (state point 3). In cases when the fluid reaches a superheated state, a third zone super-heater is required. During the above heat exchange, the temperature of the flue gas decreases from Θ_{in} to Θ_{out} . The specific heat capacity c_p of the flue gas at constant pressure is assumed to be constant. After that, the working fluid flows into the turbine and is expanded to the condensing pressure (state point 4). Then, the outlet from the turbine passes through the condenser, where heat is rejected until it becomes a saturated liquid (state point 1). After leaving the condenser, it enters the pump, where its pressure is increased to the sub-critical pressure (state point 2).

III. ENERGY ANALYSIS

Energy analysis is based on the first law of thermodynamics, which describes energy rate balance enclosing each component of the system. The control volume energy balance undergoing steady state process, without potential and kinetic energy, is expressed for each state as follows:

A. Liquid pressurization process (6-1):

This is a non-isentropic process. The power consumption of the pump can be expressed as follows:

$$\dot{W}_{pump} = \frac{\dot{m}_{wf} (h_{1,s} - h_6)}{\eta_{pump}} \quad (1)$$

B. Heat extraction process (1-4):

In this process, the heat is transferred to the working fluid across three zone heat exchanger. It can be imaginarily split into preheating section, evaporating

section, superheating section. The energy balance for the three segments is given by (2):

$$\dot{Q}_{preheater} = \dot{m}_{hf} c_p (\Theta_3 - \Theta_4) = \dot{m}_{wf} (h_2 - h_1) \quad (2)$$

$$\dot{Q}_{evaporator} = \dot{m}_{hf} c_p (\Theta_2 - \Theta_3) = \dot{m}_{wf} (h_3 - h_2) \quad (3)$$

$$\dot{Q}_{superheater} = \dot{m}_{hf} c_p (\Theta_1 - \Theta_2) = \dot{m}_{wf} (h_4 - h_3) \quad (4)$$

In cases when heat losses to surrounding are negligible, an overall heat transfer from a heat source of ORC system to a working fluid is defined as follows:

$$\dot{Q}_{in} = \dot{Q}_{heat_source} = \dot{Q}_{preheater} + \dot{Q}_{evaporator} + \dot{Q}_{superheater} \quad (5)$$

The flue gas realizes a heat at the rate of $\dot{m}_{hf} c_p (\Theta_1 - \Theta_4)$ while the working fluid absorbs heat at a rate of $\dot{m}_{wf} (h_4 - h_1)$. The heat transfer rate across a heat exchanger can be expressed as

$$\dot{m}_{hf} c_p (\Theta_1 - \Theta_4) = \dot{m}_{wf} (h_4 - h_1) \quad (6)$$

C. Power generation process state (4-5):

The power generated by the turbine during isentropic expansion is given as

$$\dot{W}_{turbine} = \dot{m}_{wf} (h_5 - h_4) \quad (7)$$

The expansion in the turbine deviates from ideal isentropic behavior by isentropic efficiency

$$\dot{W}_{turbine} = \dot{m}_{wf} (h_{5,s} - h_4) \eta_{turbine} \quad (8)$$

D. Condensation process (5-6):

In this process, the heat is rejected to cooling medium in condenser in order to condensate the working fluid and directs it in a pump intake. The amount of heat rejected is given by (10):

$$\dot{Q}_{rejected} = \dot{m}_{wf} (h_6 - h_5) \quad (10)$$

E. Net produced power:

The maximal net power output delivered by the ORC is the difference between the turbine power and the magnitude of the pump power

$$\dot{W}_{net} = \dot{W}_{turbine} - \dot{W}_{pump} \quad (11)$$

The thermal efficiency describes how efficiently the working fluid utilize the given thermal source can be calculated either via cycle efficiency (12).

$$\eta_{th} = \frac{\dot{W}_{net}}{\dot{Q}_{heat_source}} \quad (12)$$

III. EXERGY ANALYSIS

The exergy method of analysis is based on the second law of thermodynamics, which relies heavily on the use of the thermodynamic property entropy generated due to process irreversibility

Figure. 3 depicts enthalpy profiles of heat carrier and the working fluid. According to the Second Law of Thermodynamics, it is impossible to convert the whole available thermal energy into useful work. From both a thermodynamic and technical point of view, the temperature profiles depend on the properties of the working fluids such as the properties at vapor–liquid critical point, the saturation line and specific heat since they affect how well the temperature profile of the working fluid can be matched by the corresponding thermal energy source. Hence; better thermal matching between the heat source and the working fluid leads to better cycle efficiency. On the other hand, the temperature mismatching indicates that the irreversibility and exergy destruction will be inherently large across a heat exchanger (see Figure. 4). As for the finite heat source, temperature mismatching is unavoidable since it is a single phase and possesses linear temperature profile during heat transfer process [6, 19]. Thus, the exergy analysis allows pinpointing the causes of inefficiencies, locations and magnitudes of losses [20, 21]. The destroyed exergy rate is determined by the destruction of exergy during the heat transfer process in the heat extraction process. This gap can be defined as the difference between hot and working fluid and is given by (13):

$$\Delta\dot{E}x_{destruction} = \Delta\dot{E}x_{hf} - \Delta\dot{E}x_{wf} \quad (13)$$

Where the $\Delta\dot{E}x_{destruction}$ is the rate of exergy destruction, $\Delta\dot{E}x_{hf}$ is the rate of exergy transfer to the system by heat and mass flow, and $\Delta\dot{E}x_{wf}$ is the rate of exergy transfer from the system.

Here the exergy destruction $\Delta\dot{E}x_{destruction}$ can be classified as follows:

$$\Delta\dot{E}x_{destruction} = T_0 S_{generation} \geq 0 \quad (14)$$

A. Liquid pressurization process (6-1):

The exergy destruction rate in the pump is given by equation (15)

$$(\Delta\dot{E}x_{destruction})_{pump} = \dot{m}_{wf} T_0 (S_1 - S_6) = \dot{m}_{wf} (ex_1 - ex_6) \quad (15)$$

The rate of exergy transfer by mass flow can be expressed as follows:

$$\Delta\dot{E}x_{hf} = \dot{m}_{wf} (h_4 - h_1 - T_0 (S_4 - S_1)) \quad (16)$$

The rate of exergy transfer accompanying heat transfer to the system is determined by

$$\Delta\dot{E}x_{hf} = \int (1 - \frac{T_0}{T}) \delta\dot{Q}_{in} \quad (17)$$

The destroyed exergy rate for the system is given by:

$$\Delta\dot{E}x_{destruction} = \dot{Q}_{in} (1 - \frac{T_0}{T_{avg}}) - \dot{m}_{wf} (ex_4 - ex_1) \quad (18)$$

Where the thermodynamic average temperature T_{avg} can be defined as follows:

$$T_{avg} = 1 - \frac{2T_0}{T_{hf,in} + T_{hf,out}} \quad (19)$$

For each individual component, it can be expressed as follows:

$$(\Delta\dot{E}x_{destruction})_{preheater} = \dot{Q}_{in} (1 - \frac{T_0}{T_{avg}}) - \dot{m}_{wf} (ex_2 - ex_1) \quad (20)$$

$$(\Delta\dot{E}x_{destruction})_{evaporator} = \dot{Q}_{in} (1 - \frac{T_0}{T_{avg}}) - \dot{m}_{wf} (ex_3 - ex_2) \quad (21)$$

$$(\Delta\dot{E}x_{destruction})_{superheater} = \dot{Q}_{in} (1 - \frac{T_0}{T_{avg}}) - \dot{m}_{wf} (ex_4 - ex_3) \quad (22)$$

B. Power generation process state (4-5):

The exergy destruction rate in the turbine can be defined by eq. (23)

$$(\Delta\dot{E}x_{destruction})_{turbine} = \dot{m}_{wf} T_0 (S_5 - S_4) = \dot{m}_{wf} (ex_5 - ex_4) \quad (23)$$

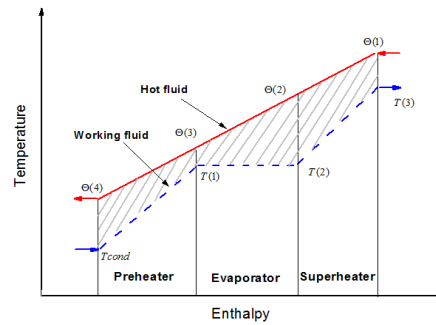


Figure. 3 T- ΔH diagram of the hot and cold composite curve.

C. Condensation process (5-6):

The exergy destruction rate in the condenser is given by:

$$(\Delta\dot{E}x_{destruction})_{condenser} = \dot{Q}_{in} (1 - \frac{T_0}{T_{L,avg}}) - \dot{m}_{wf} (ex_6 - ex_5) \quad (24)$$

In order to reflect the ability to utilize high grade waste heat into usable work, the exergy efficiency of ORC system evaluates the performance for waste heat recovery and is a measure of how close the system is to a reversibly operating system.

$$\eta_{energy} = \frac{\dot{W}_{net}}{\dot{E}x_{hf}} \quad (25)$$

IV. MODEL ESTABLISHMENT

The thermodynamic properties of the working fluid candidates are obtained from DIADEM PRO. A number of assumptions are made to simplify ORC analysis in this study. The model is assumed to be in a steady state condition with no pressure drops in connecting pipes and heat exchanger. The process of heat addition and rejection are therefore assumed to be isobaric. Changes in kinetic and potential energy of the working fluid have also been considered negligible. The expansion in the turbine and the compression by the pump were assumed to deviate from ideal isentropic behavior by isentropic efficiencies of ($\eta_{turbine} = 72\%$) and ($\eta_{pump} = 65\%$) respectively. The heat carrier fluid is modeled as flue gas at varied inlet temperatures which ranged from 543 K to 633 K with a 10 K step. It flows at steady molar flow rate 0.412 kmole/s, the specific heat capacity c_p at constant pressure was 32201 J/Kmole.K, the minimum temperature difference ΔT in the evaporator was 10 K, the condensation temperature of working fluid and the ambient temperature ($T_0=298.15$ K). The model takes into account a number of constraints which are set in agreement with those presented by [19].

A. Object function:

The net power output generated in expansion process is part of the objective function employed in the optimization process and the purpose of the optimization is to minimize the value of that objective function. The latter concerns the specific net power output of the cycle only and can be formulated in general terms as follows:

$$\min(obj - fun) = \dot{\Delta}E_{destruction} - \dot{W}_{net} \quad (26)$$

B. Optimization constraints:

To ensure that cycle parameters remain within limits that are practical and physically realizable, it is important to specify limits in the form of constraint equations.

1) Minimum approach temperature difference

The cycle calculations were carried out by constraining the minimum approach temperature difference between the heat source and the working fluid occurs at the cold end of the evaporator in order to

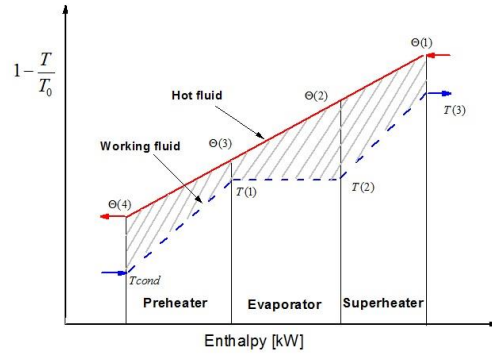


Figure. 4 Exergy composite curve of heat extraction.

prevent the violation of the second law of thermodynamics [22].

$$\Theta \left(\sum_{l=1}^n \Delta H_l^{wf} \right) - T \left(\sum_{l=1}^n \Delta H_l^{wf} \right) - \Delta T_{PP} \geq 0 \quad (27)$$

$$\Theta \left(\sum_{j=1}^n \Delta H_j^{hf} \right) - T \left(\sum_{j=1}^n \Delta H_j^{hf} \right) - \Delta T_{PP} \geq 0 \quad (28)$$

2) Temperature feasibility

Another constraint adopted in the calculations with a small difference between the saturated temperature and flue gas temperature in order to secure the subcritical conditions.

$$T_{j+1} - T_j \geq 0 \quad (29)$$

3) Turbine outlet temperature

Additional constraint is implemented to the cycle calculations to secure that the working fluid will leaves the turbine in the state of saturated vapor or superheated

$$C_{p,liq,i} (T_{3i-1} - T_0) + \Delta H_{vaporation} (T_{3i-1}) - C_{p,vap,i} (T_{turb,out,i} - T_0) \leq 0 \quad (30)$$

C. Optimization algorithms:

In order to find a globally optimal solution for organic rankine cycle with the minimum value of that objective function, two global solvers are used in the optimization process, performed by Global Search and Multi-Start. Both Global Search and Multi-Start solvers use a general class of optimization algorithms such as trust-region-reflective, active-set, interior-point and SQP in order to search within a domain to arrive at the global optimum solution. Aforementioned global solvers generate multiple start points and then unlike those classical algorithms are employed on these generated

points in order to find global optimal solution and avoid local minima. Hence, the objective function value improves its value as an approximation to the global optimum without violating any constraints.

V. RESULTS AND DISCUSSION

The Equations (1)–(25), together with boundary conditions (27) – (30) define nonlinear problem. To provide global optimality of solutions deterministic the multi start local solver method is used to solve problem for objective functions.

Figure. 5 shows the net power output curves of selected dry fluids at various inlet temperatures of the hot fluid from 543 to 633 K with a 10 K step. Among these working fluids, the results indicate that nonane exhibit the largest amount of work between 186–266 kW in the temperature range (543-573 K) while toluene assures the largest amount of work between 265-560kW beyond this range (>573) followed by ethylbenzene (260-502kW), P-xylene (250-497kW), O-xylene (243-483kW) and propylbenzene (255-466kW).

Figure. 6 and Figure. 7 show the variations of the thermal and exergy efficiency with the heat source inlet temperature respectively. Since the characteristics and process parameters (inlet temperatures, outlet temperature and the flow rate) of the flue gas are imposed; the exergy and thermal efficiencies curves have similar variation

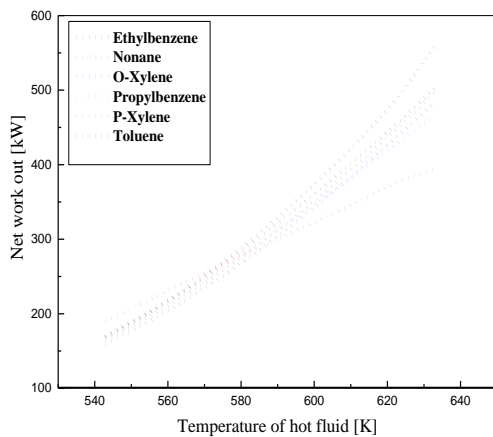


Figure. 5 The variation of net power output for different working fluids with hot fluid temperature.

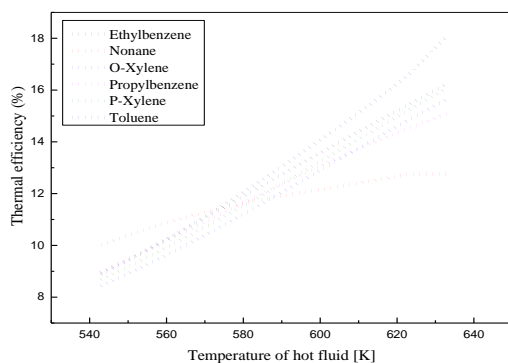


Figure. 6 The variation of thermal efficiency for different working fluids.

trends with W_{net} for fixed heat input. As a consequence, when each working fluid has higher maximal net power

output, it means that working fluid has a higher total exergy and thermal efficiency of ORC.

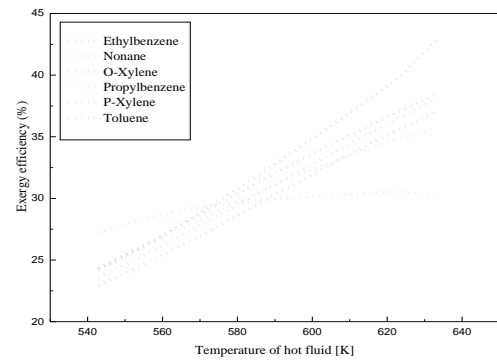


Figure. 7 The variation of exergy efficiency for different working fluids.

Among these working fluids, the results indicate that nonane exhibit the highest thermal and exergy efficiency(12%)(30%) respectively in the temperature range (543-573 K) while toluene assures the highest thermal and exergy efficiency (18%)(42.5%) beyond this range (>573) followed by ethylbenzene (16%)(3.75%), P-xylene (15.5%)(37%), O-xylene (15.5%)(36.5%) and propylbenzene (15%)(35.5%).

Generally speaking, the choice of the working fluid is of key importance in ORC applications and can greatly affect the optimal evaporating pressure in the cycle since cycle efficiency is very sensitive to evaporating pressure. In other words, the lower evaporation pressure will have a lower temperature which means that the working fluid does not extract as much heat as it would at a higher evaporating pressure (with the associated higher evaporating temperature) and would eventually have a lower thermal efficiency (Figure. 8).

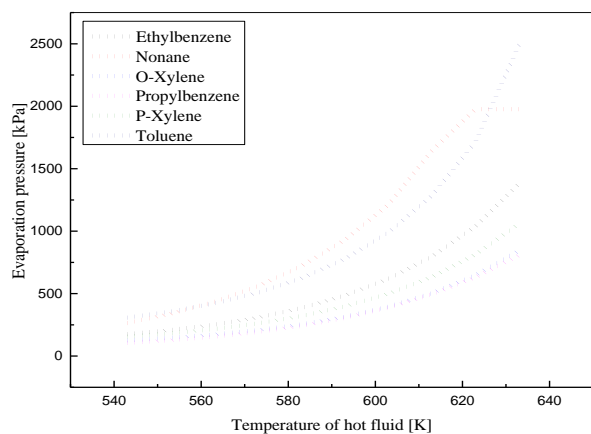


Figure. 8 The variation of evaporation pressure for different working fluid

Since the condensation temperature was constant, the condensing pressure did not change for any specific fluid regardless of the variation of the evaporation temperature. Consequently, it is obvious that an increase in the pressure difference between evaporator and condenser cause the temperature difference between working fluid and finite thermal source to decrease and the result is a reduction in the rate of entropy generation (exergy loss)

which leads to an improvement in the exergy efficiency. However, the difference value must not exceed beyond its optimal value since it will lead to a rapid increase of heat exchanger area.

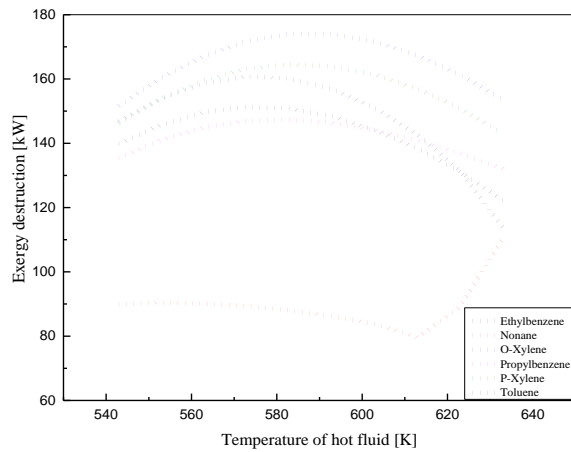


Figure. 9 The variation of exergy destruction for different working fluid

Figure. 8 and Figure. 9 show the variations of the evaporation pressure and exergy destruction with the heat source inlet temperature respectively. As it can be readily seen from these figure that propylbenzene (543K) represents significantly low evaporating pressures below the atmospheric pressure. On the other hand, toluene (2490 kPa) shows the highest evaporating pressure, followed by nonane (1977kPa), Ethylbenzene (1380kPa), P-xylene (1059 kPa) and O-xylene (843kPa). The use of fluids representing the lowest evaporating pressures might limit their usage since these fluids can be considered to be more potential for ORC systems.

VI. CONCLUSION

The aim of this study was to investigate the performance of subcritical ORC operating at various inlet temperatures of the flue gas from 543 to 633 K with hydrocarbons as a potential working fluid. This analysis was carried out basing on the basic thermodynamic theory, and parameters such as net power output, exergy efficiency, thermal efficiency, which were evaluated and compared among working fluid candidates. Based on this analysis, the most suitable fluid candidates were nominated and ranked according to the proposed screening criteria parameters. Model calculations were performed at fixed condenser temperature, isentropic turbine efficiency (72%), isentropic pump efficiency (65%) and different evaporation pressures and temperatures. The results were obtained by adopting evaporation pressure slightly lower than the critical pressure of the fluid. Its lowest value is set equal to the condenser pressure which is determined from condensing temperature. Its highest value is set equal to the saturation pressure corresponding to the saturation temperature in order to limit the ORC being a supercritical cycle and to represent cycle efficiencies in the vicinity of maximum efficiency that can be achieved with a subcritical process. For ORC processes operating at various inlet temperatures of hot fluid from 543 to 573K, the overall

ranking of the working fluids for power output optimization including heat transfer to the ORC depicts that linear alkanes such as nonane can be better matched to the finite thermal energy source. Beyond this range (573-633K), aromatic hydrocarbons such as toluene, ethylbenzene, P-xylene, O-xylene, Propylbenzene exhibit a superior performance and they represent comparably similar efficiencies with high cycle efficiency, exergy efficiency, net power output, and comparably high evaporating pressure, with only occasional slight differences between them. Under saturated expansion, the thermal efficiency is increased with respect to greater evaporation pressure. Greater evaporation pressure leads to less irreversibility rate.

Nomenclature

m	mass flow rate (kg/s)
h	specific enthalpy (kJ/kg)
c_p	heat capacity in heat exchanger (kW)
\dot{W}	power (kW)
\dot{Q}	heat rate during the heat addition process (kW)
Θ	temperature of hot fluid (K)
T	temperature of working fluid (K)
$e\dot{x}$	exergy flow rate (kW)
s	Specific entropy (kJ/Kg.K)
P	pressure (kPa)
C_{pliq}	average specific heat capacity for enthalpy change for liquid in kJ/kmol.K
C_{pvap}	average specific heat capacity for enthalpy change for vapor in kJ/kmol.K
ΔH_{vap}	latent heat in kW/kmol

Greek letters

η efficiency (%)

Δ gradient

Subscripts

0 reference condition

hf hot fluid

wf working fluid

sat saturation

evap evaporator

pp pinch point temperature difference

Turb,out outlet from turbine

p pump

t turbine

th thermal efficiency

net net power output

c critical

ex exergy efficiency

Acronyms

ORC Organic Rankine Cycle

Indices

i index for pressure level

<i>i</i>	index for enthalpy intervals for working fluid
<i>j</i>	index for enthalpy intervals for hot fluid
<i>n</i>	Polytropic index

REFERENCES

- [1] J. Bao, L. Zhao, "A review of working fluid and expander selections for organic Rankine cycle," *Renewable and sustainable energy reviews*, vol.24. pp. 325-342,(2013).
- [2] S. Quoilin, M. Van Den Broek, S. Declaye, P. Dewallef, V. Lemort, "Techno-economic survey of Organic Rankine Cycle (ORC) systems," *Renewable and sustainable energy reviews*, vol.22. pp. 168-186,(2013).
- [3] H. Chen, D.Y. Goswami, E.K. Stefanakos, "A review of thermodynamic cycles and working fluids for the conversion of low-grade heat," *Renewable and sustainable energy reviews*, vol.14. pp. 3059-3067,(2010).
- [4] F. Vélez, "Selecting working fluids in an organic Rankine cycle for power generation from low temperature heat sources," *Dyna*, vol.81. pp. 173-180,(2014).
- [5] M.A. Siddiqi, B. Atakan, "Alkanes as fluids in Rankine cycles in comparison to water, benzene and toluene," *Energy*, vol.45. pp. 256-263,(2012).
- [6] T. Ho, S.S. Mao, R. Greif, "Comparison of the Organic Flash Cycle (OFC) to other advanced vapor cycles for intermediate and high temperature waste heat reclamation and solar thermal energy," *Energy*, vol.42. pp. 213-223,(2012).
- [7] G. Angelino, P.C. Di Paliano, "Multicomponent working fluids for organic Rankine cycles (ORCs)," *Energy*, vol.23. pp. 449-463,(1998).
- [8] M.A. Qyyum, A. Naquash, W. Ali, J. Haider, A.A. Noon, M. Rehan, A.-S. Nizami, M. Yasin, M. Lee, "Process Systems Engineering Evaluation of Prospective Working Fluids for Organic Rankine Cycles Facilitated by Biogas Combustion Flue Gases," *Frontiers in Energy Research*, vol.9. pp. 135,(2021).
- [9] R.A. Victor, J.-K. Kim, R. Smith, "Composition optimisation of working fluids for Organic Rankine Cycles and Kalina cycles," *Energy*, vol.55. pp. 114-126,(2013).
- [10] S. Lecompte, H. Huisseune, M. Van Den Broek, B. Vanslambrouck, M. De Paepe, "Review of organic Rankine cycle (ORC) architectures for waste heat recovery," *Renewable and sustainable energy reviews*, vol.47. pp. 448-461,(2015).
- [11] B.F. Tchanche, M. Pétrissans, G. Papadakis, "Heat resources and organic Rankine cycle machines," *Renewable and Sustainable Energy Reviews*, vol.39. pp. 1185-1199,(2014).
- [12] V. Apostol, H. Pop, A. Dobrovicescu, T. Prisecaru, A. Alexandru, M. Prisecaru, "Thermodynamic analysis of ORC configurations used for WHR from a turbocharged diesel engine," *Procedia Engineering*, vol.100. pp. 549-558,(2015).
- [13] A.A. Lakew, O. Bolland, "Working fluids for low-temperature heat source," *Applied Thermal Engineering*, vol.30. pp. 1262-1268,(2010).
- [14] H.M. Hettiarachchi, M. Golubovic, W.M. Worek, Y. Ikegami, "Optimum design criteria for an organic Rankine cycle using low-temperature geothermal heat sources," *Energy*, vol.32. pp. 1698-1706,(2007).
- [15] S. Quoilin, S. Declaye, B.F. Tchanche, V. Lemort, "Thermo-economic optimization of waste heat recovery Organic Rankine Cycles," *Applied thermal engineering*, vol.31. pp. 2885-2893,(2011).
- [16] B.-T. Liu, K.-H. Chien, C.-C. Wang, "Effect of working fluids on organic Rankine cycle for waste heat recovery," *Energy*, vol.29. pp. 1207-1217,(2004).
- [17] N.B. Desai, S. Bandyopadhyay, "Process integration of organic Rankine cycle," *Energy*, vol.34. pp. 1674-1686,(2009).
- [18] R. Rayegan, Y. Tao, "A procedure to select working fluids for Solar Organic Rankine Cycles (ORCs)," *Renewable Energy*, vol.36. pp. 659-670,(2011).
- [19] M.Z. Stijepovic, A.I. Papadopoulos, P. Linke, A.S. Grujic, P. Seferlis, Design of multi-pressure organic rankine cycles for waste heat recovery in site utility systems, in: *Computer Aided Chemical Engineering*, vol. 33, Elsevier, 2014, pp. 109-114.
- [20] M. Bendig, F. Maréchal, D. Favrat, "Defining "Waste Heat" for industrial processes," *Applied Thermal Engineering*, vol.61. pp. 134-142,(2013).
- [21] S. Safarian, F. Aramoun, "Energy and exergy assessments of modified Organic Rankine Cycles (ORCs)," *Energy reports*, vol.1. pp. 1-7,(2015).
- [22] M.Z. Stijepovic, A.I. Papadopoulos, P. Linke, A.S. Grujic, P. Seferlis, "An exergy composite curves approach for the design of optimum multi-pressure organic Rankine cycle processes," *Energy*, vol.69. pp. 285-298,(2014).